Impact echo scanning for imaging of grout defects to mitigate corrosion in post-tensioned bridge ducts

A.T. Balkema, G. Westers, L.D. Olson, Y. Tinkey & A. Gibson
Olson Engineering, Inc.

ABSTRACT: This paper focuses on imaging and scanning technology based on the rolling Impact Echo Scanning (IES) method. The background of the Impact Echo technique and its implementation with a rolling scanning transducer are discussed herein. 2D and 3D displays using the amplitude normalization and thickness surface plot techniques including typical results in time and frequency domains from a US National Cooperative Highway Research Program (NCHRP) research project are included with this paper along with a case history from a post-tensioned segmental bridge. Impact Echo is generally used to either determine the internal condition of the concrete structures or measure the thickness of the structures. The rolling transducer in the IE Scanner expedites the IE test process by allowing for rapid, near-continuous testing.
In field bridge investigations, ducts are typically located using Ground Penetrating Radar (GPR). Then an Impact Echo Scanner was used to scan along and across ducts for internal grout condition evaluations. The results from Impact Echo scanning were processed with an automatic filtering including a bandpass filter to remove ambient noise and a bandstop filter to remove the undesired rolling noise frequency. This technique produced good accuracy in locating voids in steel ducts in the bridge. A sensitivity study was conducted for Styrofoam voids of varying size in 100 mm diameter ducts in a full-scale bridge girder in the NCHRP research. Honeycomb void was also imaged with IES in the research. The 2D display Impactechogram and 3D display of surface plot data helps in data interpretation by enhancing the visualization and interpretation of the test results. The NDE results from IES tests of post-tensioned steel ducts in a post-tensioned segmental bridge are also discussed. Destructive drilling and further inspection by videoscope were performed on these ducts to confirm their actual conditions. Results from the IES show good agreements with the results from the videoscope observations in drillholes.

1. INTRODUCTION

This paper discusses the experimental results of impact-echo tests using a rolling impact-echo scanning system in terms of its ability to detect and image discontinuities in post-tensioned ducts of a mock-up U shaped bridge girder. Comparisons of the interpretation and the actual design conditions of the post-tensioned ducts inside the bridge girder are presented. The impact-echo results are presented in a three-dimensional fashion using thickness surface plots to provide better visualization and interpretation of the internal conditions of the girder. In addition, actual NDE results from post-tensioned steel ducts in a bridge are discussed. Ground Penetrating Radar (GPR) was first used to locate the ducts. Next, IE Scanning was done to locate anomalies indicative of void. Drilling and borescope examination were used to confirm voids.

The impact-echo tests were performed with a scanner which further expedites the impact-echo test process by allowing for rapid, near-continuous testing and true “scanning” capabilities to test concrete structures. The paper summarizes the general background of the impact-echo technique and the impact-echo scanner. Descriptions of the mock-up specimen used in the experiment and the discussion of the results from the impact-echo scanner are presented herein. Results from destructive coring and further inspection by videoscope are included in this paper for comparison purposes.

2. BACKGROUND OF THE IMPACT ECHO TECHNIQUE

The impact-echo test involves dynamically exciting a concrete structure with a small mechanical impactor and measuring the reflected wave energy with a displacement transducer. The resonant echoes in the displacement responses are usually not apparent in the time domain, but are more easily identified in the frequency domain. Consequently, amplitude spectra of the displacement responses are calculated by performing a Fast Fourier Transform (FFT) analysis to determine the resonant echo peaks. The relationship among the depth frequency peak f the compression wave velocity V_P and the echo depth *D* is expressed in the following equation:

$$D = \beta V_p/(2*f) \quad \textbf{(1)}$$

Here, β is a factor which varies based on geometry and was found by theoretical modeling to be equal to 0.96 for a slab/wall shape (Sansalone and Streett, 1997) which was theoretically verified based on Lamb wave theory recently (Gibson and Popovics, 2003).

3. IMPACT ECHO SCANNER

The impact-echo rolling scanner was first conceived by the first author of this paper and researched and developed as a part of a US Bureau of Reclamation prestressed concrete cylinder pipe integrity research project (Sack and Olson, 1995). This technique is based on the impact-echo method (Sansalone and Streett, 1997; ASTM, 2004). In general, the purpose of the impact-echo test is usually to either locate delaminations, honeycombing or cracks parallel to the surface or to measure the thickness of the structures (concrete beams, floors or walls). To expedite the impact-echo testing process, an impact-echo scanning device has been developed with a rolling transducer assembly incorporating multiple sensors, attached underneath the test unit. When the test unit is rolled across the testing surface, an optocoupler on the central wheel keeps track of the distance. This unit is calibrated to impact and record data at intervals of nominally 25 mm (1 in.). If the concrete surface is smooth, a coupling agent between the rolling transducer and test specimen is not required. However, if the concrete surface is rough, water can be used as a coupling material. A comparison of the impact-echo scanner and the point by point impact-echo unit is shown in Figure 1. Typical scanning time for a line of 4 m (157 in.), approximately 150 points, is 60 s. In an impact-echo scanning line, the resolution of the scanning is about 28 mm (1.09 in.) between impact points. Data analysis and visualization was achieved using impact-echo scanning software developed by the first author for a National Cooperative Highway Research Program Innovations Deserving Exploratory Analysis (NCHRP-IDEA) grant for stress wave scanning of post-tensioned bridges. Raw data in the frequency domain were first filtered using a Butterworth filter with a band-pass range of 2 to 20 kHz. Due to some rolling noise generated by the impact-echo scanner, a band-stop filter was also used to remove the undesired rolling noise frequency. Automatic and manual picks of dominant frequency were performed on each data spectrum and an impact-echo thickness was calculated based on the selected dominant frequency. A three-dimensional plot of the condition of the large concrete bridge web wall was generated by combining the calculated impact-echo thicknesses from each scanning line. The three-dimensional results can be presented in either color or grayscale.

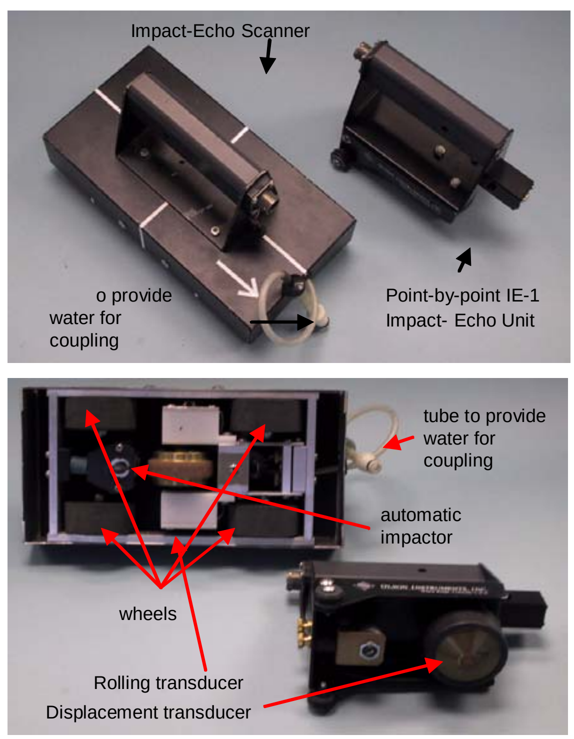

Figure 1. Impact-Echo Scanner Unit and Point-by-Point Impact-Echo Unit

4. GENERAL DESCRIPTION OF THE MOCKUP GIRDER AND DEFECTS

4.1 Description of the Mockup Girder

A full scale pre-cast bridge girder (U-shaped) was donated to the research team for use in grout defect sensitivity studies as part of an ongoing research project funded by the NCHRP-IDEA program. The length of the girder is 30.48 m (100 ft) with a typical wall thickness of 25.4 cm (10 in). There were four empty metal ducts (10.16 cm or 4 inches in diameter) inside each wall (Figure 2). The west end of the girder (6.1 m or 20 ft long) was selected for this study. Stepped and tapered Styrofoam rods (10.16 cm or 4 inches in diameter) were inserted into the ducts before grouting to form internal voids with sizes ranging from small to full diameter voids.

4.2 Styrofoam Defects

Modified Styrofoam rods (10.16 cm or 4 inches in diameter) were inserted into the ducts before grouting to form internal voids with sizes ranging from small to almost full diameter voids. Figure 3 shows a Styrofoam rod being inserted into the top duct of the north wall. A wire (1/8 inch or 3 mm in diameter) was bent to form a leg for the Styrofoam rod so that the foam would be positioned on the roof of the duct, which simulates the real world grout defects formed by air and water voids. Smaller defects were glued directly to the roof of the duct since they were too thin for the wire leg. The defect sizes are presented in Table 1 in terms of their circumferential perimeter and depth lost. The defect designs are presented in Table 1 for all four ducts in the South web wall. The actual percentage of circumferential perimeter and diameter depth lost due to the defect are shown in the underlined numbers placed directly above the defects in Figure 4.

Figure 2. U-Shaped Bridge Girder with Eight Empty Ducts

Figure 3 – Styrofoam rods being inserted into the duct

Table 1 – Styrofoam Defect Sizes

Defect ID	Circumferencial Lost (cm, in)	Depth Lost (cm, in)	Percentage Lost in Circumferencial Permineter (%)	Percentage Lost in Depth (%)
1	5.08, 2	0.635, 0.25	16	6
2	7.72, 3	1.36, 0.535	24	13
3	10.16, 4	2.34, 0.92	32	23
4	12.7, 5	3.48, 1.37	40	34
5	15.95, 6.28	5.08, 2	50	50
6	19.23, 7.57	6.68, 2.63	60	66
7	21.77, 8.57	7.82, 3.08	68	77
8	24.31, 9.57	8.79, 3.46	76	87
9	26.85, 10.57	9.52, 3.75	84	94

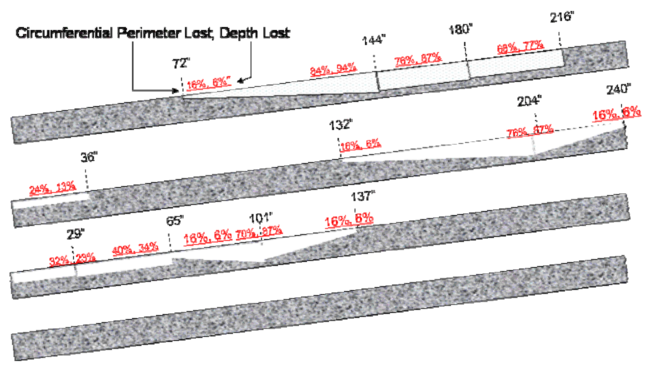

Figure 4. Actual Grout Defect in the South Wall in 10.16 cm (4 in) Metal Ducts

5. EXPERIMENTAL RESULTS FROM THE MOCK-UP GIRDER

5.1 Interpretation of Impact Echo Data

Localization of grouting discontinuities through impact-echo in the mockup girder was based on an analysis of variations in the impact-echo frequency. A direct echo from the void or duct wall, measured as an impact-echo frequency corresponding to the depth of the discontinuity (given by the formula D = v/2f where V_P = IE compression wave velocity and f =frequency), has not yet been observed with the scanner. The only IE-based indication of the presence of well-grouted, filled tendon ducts is the apparent minor increase in apparent wall thickness over such a duct (typically on the order of 12.7 mm or 0.5 in or less). Grouting defects cause a more significant increase of the apparent wall thickness in IE results as shown herein. This is in accordance with the interpretation of the impact-echo signal as a resonance effect, rather than a reflection of a localized acoustical wave.

5.2 Discussion of Impact Echo Results

The Impact Echo tests were performed using a rolling scanner at 1, 3 and 8 days after the grouting process was completed. This paper includes results from the South wall testing 3 days after the grouting of the ducts was completed. Ultrasonic Pulse Velocity tests were performed on a sample of the grout placed on-site in a 40.64 cm (16 in) long duct. The grout velocity at 3 days old was 11,400 ft/sec, indicative of solid grout. The results from the IE scanning of the South wall is presented in a thickness tomogram fashion as shown in Figures 5 - 8. Figures 5 – 8 show the experimental results compared with the actual defect designs of the ducts. The drawing of the actual defect design is placed above the experimental results of the duct for comparison purposes.

South Wall – Top Duct: The IE results from the South Wall with the actual defect design of the top duct placed above the IE results of the top duct are shown in Figure 5. The results are interpreted to indicate that the grout defect started to appear at a length of 1.93 m (76 in) and becomes clearly evident at length of 2.92 m (115 in) from the west end of the duct. The location that the defect starts to appear corresponds to void with 11% depth lost or 20% circumferential perimeter lost. The location that the grout defect become more evident corresponds to void with 59% depth lost or 57% circumferential contact diameter lost. The dominant frequency of the fully grouted duct is approximately 6.4 kHz, resulting in an apparent impact-echo thickness of 28.37 mm (11.17 in.). The dominant frequency shifted to approximately 5.37 kHz for an empty duct, which corresponds to an apparent impact-echo thickness of 34.0 cm (13.4 in.). This is a relatively large thickness shift of over 30% compared to the nominal thickness of the wall. The interpretation of the impact-echo scanner results, however, shows a downshift in frequencies from lengths of 5.49 to 6.1 m (216 to 240 in), indicating voids at duct locations where no discontinuities were intentionally placed. It is likely that grout did not flow into the east end due to the big voids in front of it. Radiographic tests will be performed in the future to verify the design versus actual conditions of the simulated defects.

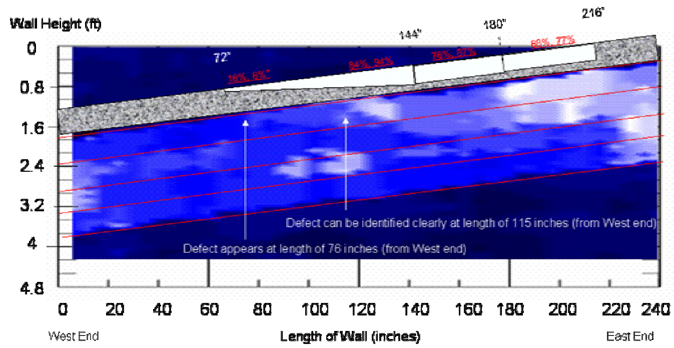

Figure 5. IE Results from the South Wall with Actual Design Defects of Top Duct

South Wall – Second Duct from Top: Review of Figure 6 shows that there are three grout defect zones. The first grout defect zone correlates with the end defect (13% depth lost or 24% circumferential lost). The second defect zone shows minor grout problem from lengths of 0.91 – 1.67 m (36 – 66 in) from the west end of the duct. However, there is no actual defects placed in this area. Radiography is required to confirm the realization of defect designs. The third defect zone appears at a length of 3.35 m (132 in) which corresponds to defect of 9% in depth lost or 18.5% in circumferential lost. The most apparent grout defect appears at a length of 5.18 m (204 in) corresponding to the location of the largest Styrofoam in the duct (87% depth lost or 76% circumferential perimeter lost). Similar to the results from the top duct, the interpretation of the impact-echo scanner results, however, shows a downshift in frequencies from lengths of 5.18 to 6.1 m (204 to 240 in), indicating major voids at duct locations where actual defect shape tapers down toward the east end. It is likely that grout did not flow in to the east end due to the big voids in front of it.

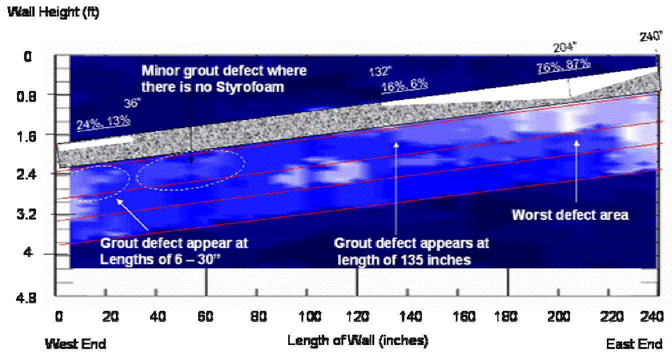

Figure 6 – IE Results from the South Wall with Actual Design Defects of Second Duct

<u>South Wall – Third Duct from Top:</u> Figure 9 shows three zones of grout defects. The first area is located at the west end where Styrofoam Defect ID# 3 (see Table 1) is in place. However, the IE results show that the duct is fully grouted between lengths of 0.45 – 2.13 m (18 – 84 in) from the west end where there are actual Styrofoam defects placed in these locations. The grout defect appears again between lengths of 2.13 – 3.2 m (84 – 126 in). The starting location of the second defect zone corresponds to actual defect of 49% depth lost or 48% circumferential lost. The end location of the defect zone corresponds to an actual defect of 30% depth lost or 34% circumferential perimeter grout contact lost. The interpretation of the impact-echo scanner results, however, shows a downshift in frequencies from lengths of 3.48 – 6.1 m (137 to 240 in), indicating minor to major voids at duct locations where no actual Styrofoam defect is in place. Radiography is required to confirm the actual final location of Styrofoam voids.

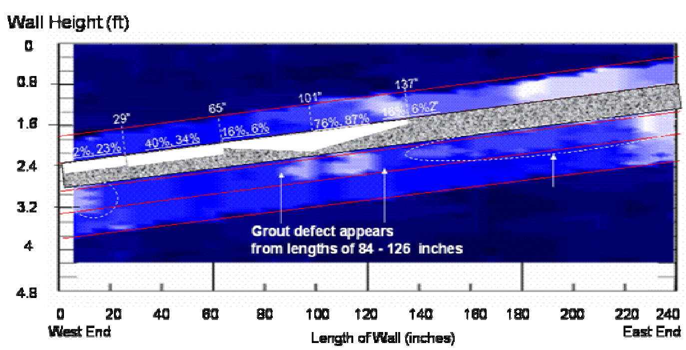

Figure 7. IE Results from the South Wall with Actual Design Defects of Third Duct

<u>South Wall – Bottom Duct:</u> There are no Styrofoam voids placed inside the bottom duct and it is fully grouted. However the interpretation of the impact-echo scanner results shows a downshift in frequencies from a length of 5.59 m (220 in) to the east end, indicating major voids. IE results of the bottom duct compared to the actual design of the bottom duct are shown in Figure 8. Review of Figures 5 – 8 shows similar results toward the east end of the duct regardless of the presence of the Styrofoam void. It is likely that the grout levels off toward the east end of the ducts due to duct inclinations.

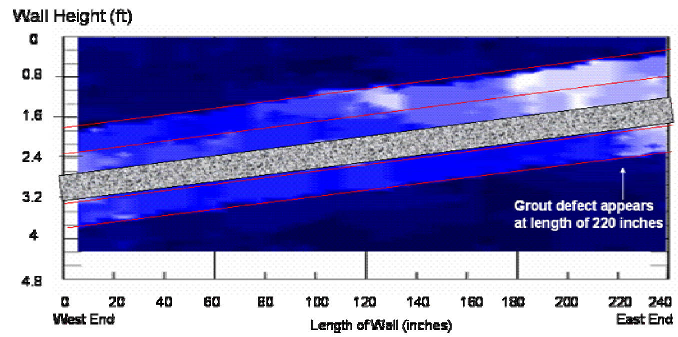

Figure 8. IE Results from the South Wall with Actual Design Defects of Bottom Duct (Completely Grouted Duct)

6. RESULTS FROM UNGROUTED DUCTS FROM A POST-TENSIONED CABLE STAYED BRIDGE

This section discusses Impactechogram results from impact echo scanning on a cable stayed post-tensioned bridge. The typical thickness of the wall section was 30 cm (12 in.) with four steel ducts inside. The ducts were first located with ground penetrating radar. Impact-echo scanning was used to evaluate the internal grout condition of four ducts in a box girder which were also destructively investigated. The IE scans were performed in such a way as to cross all four ducts vertically and along each duct laterally. Destructive coring tests and further inspection using a videoscope were performed to observe the actual condition of all four ducts. From the videoscope results, the top duct was partially filled with water, the second duct was fully grouted and the third and the bottom ducts were completely empty (see Figure 9). An impactechogram from vertical impact echo scanning across the four ducts is presented in Fig. 9. The picture inside the empty duct (bottom duct) captured from a videoscope is shown in Figure 10. Review of Fig. 9 shows that the Impact Echo results can be used effectively to identify internal conditions of the grouted ducts in the fully grouted and empty condition. However, the impact-echo scanning was not able to identify the water-filled condition. This is likely because compressional waves can travel through water resulting in conditions more similar to those of the fully grouted ducts. More experimental research is planned with an impactor with a shorter contact time (that generates higher frequency).

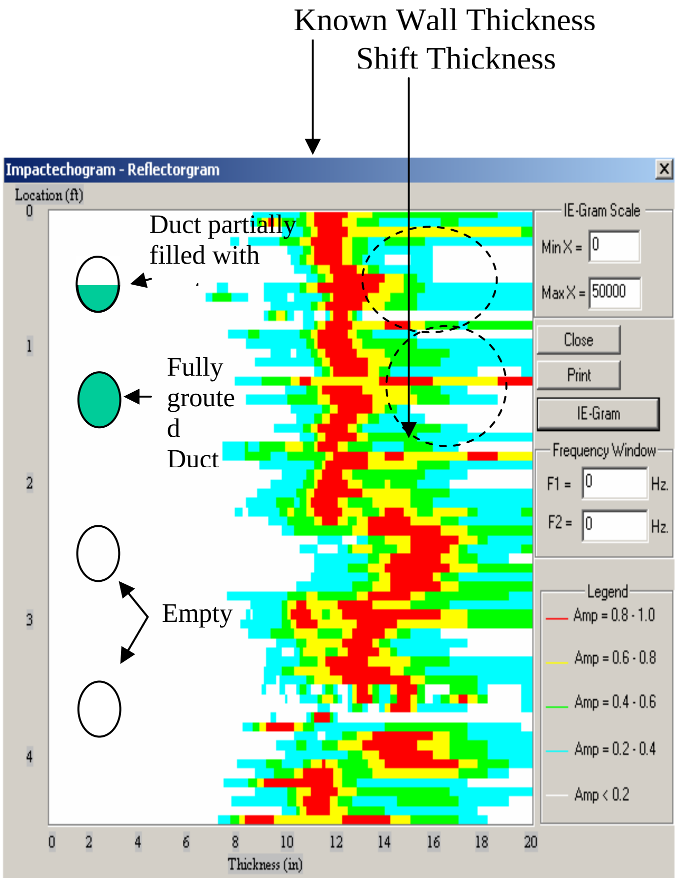

Fig. 9 – Impactechogram from IE scanning across ducts of known conditions in a Cable Stayed Bridge

Figure 10. Voids inside the Bottom Duct (from Videoscope)

REFERENCES

ASTM C1383 "Test Method for Measurement P-Wave Speed and the Thickness of Concrete Plates Using the Impact-Echo Method".

Gibson, A. and Popovic, J. 2005. "Lamb Wave Basis for Impact-Echo Method Analysis" *Journal of Engineering Mechanics*, Vol. 131, No. 4, pp. 438-443

Sansalone, M. J. and Streett, W. B., 1997. Impact-Echo Nondestructive Evaluation of Concrete and Masonry. ISBN: 0-9612610-6-4, Bullbrier Press, Ithaca, N. Y..

Sack, D. and Olson, L. D. , 1995. "Impact-Echo Scanning of Concrete Slabs and Pipes. Advances in Concrete Technology," the 2nd CANMET/ACI Intl. Symposium, Las Vegas, NV, pp. 683-692.

Tinkey, Y, Olson, L.D. and Wigenhauser, H., 2005. "Impact Echo Scanning for Discontinuity Detection and Imaging in Posttensioned Concrete Bridges and Other Structures", Materials Evaluation, vol. 1, no. 1, pp. 64-69.